Pressure effect on the magnetic properties of electron-doped $Sm_{0.1}Ca_{0.9-y}Sr_yMnO_3$ (y = 0–0.3) manganites

2006 J. Phys.: Condens. Matter 18 9201

(http://iopscience.iop.org/0953-8984/18/40/006)

INSTITUTE OF PHYSICS PUBLISHING JOURNAL OF PHYSICS: CONDENSED MATTER

J. Phys.: Condens. Matter **18** (2006) 9201–9214 doi:10.1088/0953-8984/18/40/006

Pressure effect on the magnetic properties of electron-doped $Sm_{0.1}Ca_{0.9-y}Sr_yMnO_3$ ($y = 0$–0.3) manganites

V Markovich[1], I Fita[2,3], R Puzniak[2], C Martin[4], A Wisniewski[2], S Hébert[4], A Maignan[4] and G Gorodetsky[1]

[1] Department of Physics, Ben-Gurion University of the Negev, 84105 Beer-Sheva, Israel
[2] Institute of Physics, Polish Academy of Sciences, Aleja Lotnikow 32/46, 02-668 Warsaw, Poland
[3] Donetsk Institute for Physics and Technology, National Academy of Sciences, R Luxemburg Street 72, 83114 Donetsk, Ukraine
[4] Laboratoire CRISMAT, UMR 6508 ENSICAEN/CNRS, 14050 Caen cedex 4, France

E-mail: markoviv@bgu.ac.il

Received 9 July 2006, in final form 28 August 2006
Published 22 September 2006
Online at stacks.iop.org/JPhysCM/18/9201

Abstract

Magnetic properties of polycrystalline $Sm_{0.1}Ca_{0.9-y}Sr_yMnO_3$ ($y = 0$–0.3) samples have been investigated in the temperature range 5–250 K, magnetic fields up to 16 kOe and under hydrostatic pressures up to 11 kbar. The studies involved sequential measurements of zero field cooled (ZFC) magnetization and measurements of magnetization upon cooling in the same magnetic field (FCC). The low-doped group ($y = 0$–0.1) exhibits magnetic phase separation below $T_N \approx T_C \approx 100$–110 K, consisting of ferromagnetic (FM) clusters embedded in an antiferromagnetic (AFM) G-type matrix. Magnetization and ac-susceptibility measurements of this group of materials indicate features reminiscent of a cluster glass-like state, below T_C. It was found that the volume fraction of the FM phase at 10 K decreases with increasing y from 28% for $Sm_{0.1}Ca_{0.9}MnO_3$ to 18% for $Sm_{0.1}Ca_{0.8}Sr_{0.1}MnO_3$. It was found that an applied pressure enhances T_C with a pressure coefficient of $dT_C/dP \approx 0.4$–0.5 K kbar^{-1}. The low-temperature magnetization at this doping range ($y = 0$–0.1) depends on pressure only slightly, except for the case of $Sm_{0.1}Ca_{0.8}Sr_{0.1}MnO_3$, where an applied pressure enhances the FM phase volume considerably. Samples with $y = 0.2$ and 0.3 exhibit a heterogeneous spin configuration in their ground state, consisting of a C-AFM phase and a G-AFM phase with a very weak FM moment. The temperature of transition from the paramagnetic to the C-AFM state is almost insensitive to applied pressure, whereas the lower transition temperature to the G-AFM state increases slightly under pressure. It was found also that an applied pressure considerably reduces the FM correlations in the paramagnetic phase as well as the FM component of the G-AFM state.

(Some figures in this article are in colour only in the electronic version)

1. Introduction

The manganese oxides with a general composition $RE_{1-x}AE_xMnO_3$, where RE and AE are rare- and alkaline-earth ions respectively, have been actively investigated over the past decade because of the colossal magnetoresistance (CMR) effect observed for the compounds with $x \approx 0.3$. The attractive properties of these materials have been attributed to the electronic complexity arising from the strong competition between charge, orbital, lattice, and magnetic degrees of freedom [1, 2]. It is well accepted that the double exchange (DE) ferromagnetic interaction occurs via the hopping of spin-polarized e_g electrons, between Mn^{3+} and Mn^{4+} [1]. This interaction also accounts for the electronic phase separation (PS) and for the formation of FM metallic (FMM) clusters in the antiferromagnetic (AFM) matrix. In most manganite systems, the FMM phase occurs in the hole-doped regime $x_C < x < 0.5$, where x_C is a percolation threshold. Electron-doped manganites ($x > 0.5$) are dominated by charge ordering (CO) and do not show the pure FMM ground state at all.

The properties of phase-separated manganites are governed to a large extent by the averaged radii of the A-site cations, r_A, of the ABO_3 perovskite structure and their disordered distribution. As has been argued in recent theoretical and experimental studies [3–6], the stability of the FM phase as well as the charge and orbital ordered phases are strongly affected by the presence of cation disorder. Even small fluctuation of cation disorder may result in a large shift of the transition temperature T_C of the FM phase and may change the phase diagram [6, 7]. As shown by Rodriguez-Martinez and Attfield [7], the magnitude of the cation disorder arising from a solid solution of RE and AE can be evaluated by the variance of the ionic radii, $\sigma^2 = \sum_i (x_i r_i^2 - r_A^2)$, where x_i and r_i are the fractional occupancies and the effective ionic radii of the RE and AE cations, respectively.

It was found that manganites $RE_{1-x}Ca_xMnO_3$, where RE = Sm [8–10], La [11–15], Pr [15, 16], Nd [16, 17], Dy [15], Gd [16, 17], Eu [16], Ho [16], and Y [17], exhibit in the electron doping regime the largest FM fraction around $x_{max} \sim 0.9$. At this doping, the magnetization of the FM fraction is maximal and reaches a value of about ~0.5–1 μ_B/f.u. at low temperatures. Systematic studies of magnetic and transport properties of $RE_{1-x}Ca_xMnO_3$ (RE = La, Nd, Pr, Eu, Gd, Y) have shown that higher values of x_{max} are accompanied by smaller values of r_A [16, 17]. It was also confirmed [2, 16] that the PS in these manganites increases significantly with increasing σ. Magnetic and neutron powder diffraction studies of $Sm_{0.1}Ca_{0.9}MnO_3$ [9] and $La_{0.1}Ca_{0.9}MnO_3$ [12–14] have shown a coexistence of FM clusters with an AFM G-type matrix.

In the case of $Sm_{0.1}Ca_{0.9}MnO_3$, an orthorhombic unit cell of $Pnma$ space group of a perovskite structure was observed in a wide temperature range of 2–300 K [9]. The FM and AFM phases emerge at about 110 K. At $T = 10$ K, $\mathbf{m}(G\text{-AFM}) = 2.1\ \mu_B$/Mn and $\mathbf{m}(\text{FM}) = 1.17\ \mu_B$/Mn, where $\mathbf{m}$ symbolizes the magnetic moments of the AFM G-type phase or the FM phase. Interestingly, the low-temperature magnetization $M(H)$ curve at $T = 4.2$ K does not show any indication of saturation even in a very high magnetic field H of 350 kOe [18].

It should be noted that the effect of pressure (P) on the magnetic properties of hole-doped samples of $RE_{1-x}Ca_xMnO_3$ manganites was the subject of a number of investigations (see [19–26] and references cited therein), whereas studies of the effect of pressure on magnetic properties in the low-electron-doped regime are quite scarce [27–29]. To the best of our knowledge, there are barely any studies of charge ordered $Sm_{0.2}Ca_{0.8}MnO_3$ [28] and $La_{0.2}Ca_{0.8}MnO_3$ [29] or $Y_{1-x}Ca_xMnO_3$ [27], $Sm_{1-x}Ca_xMnO_3$ ($0.85 \leqslant x \leqslant 0.95$) [27] and $La_{0.1}Ca_{0.9}MnO_3$ [29] having competing FM and AFM phases. In the case of $Sm_{0.1}Ca_{0.9}MnO_3$ [27] and $La_{0.1}Ca_{0.9}MnO_3$ [29], only a relatively weak pressure dependence of T_C (~0.5–0.6 K kbar^{-1}) was observed. On the other hand, the FM component of the G-AFM

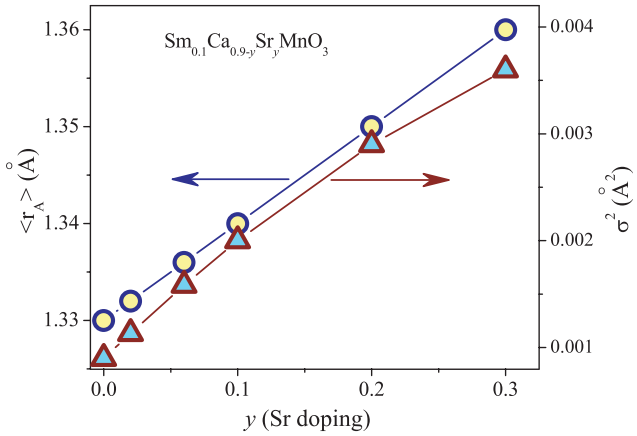

Figure 1. Variation of r_A and σ^2 with y in $Sm_{0.1}Ca_{0.9-y}Sr_yMnO_3$.

phase of $La_{0.1}Ca_{0.9}MnO_3$ was found to be very sensitive to applied pressure, e.g. a pressure of $P \approx 11$ kbar doubles the spontaneous magnetization at $T = 5$ K.

In this work we report on the magnetic measurements of electron-doped $Sm_{0.1}Ca_{0.9-y}Sr_y$ MnO_3 ($y = 0$–0.3) manganites under pressure, keeping a constant carrier concentration of 0.1 electron per Mn ion and varying r_A and σ [2]. The pressure effect on the magnetic transition temperatures and magnetic interactions is discussed.

2. Experiment

Measurements of magnetization were carried out on polycrystalline samples, prepared by a standard ceramic route in air, with intermediate crushing and heating [30]. The oxygen stoichiometry was checked by iodometric titration. It was found from chemical titration that the oxygen content is equal to 3.00 for all the samples within an experimental error of ± 0.02. The purity of the samples has been checked by x-ray powder diffraction at room temperature. Additionally, all of the samples were characterized by electron diffraction (ED) and energy dispersive spectroscopy (EDS). Analyses confirm that the cationic compositions are homogeneous and close to the nominal ones. The sample $Sm_{0.1}Ca_{0.6}Sr_{0.3}MnO_3$ was also characterized by neutron diffraction. The x-ray data at room temperature were found to be compatible with an orthorhombic unit cell of a *Pnma* space group of a perovskite structure for all the samples with $0 \leqslant y \leqslant 0.3$. The lattice parameters of $Sm_{0.1}Ca_{0.9}MnO_3$ with $c < b\sqrt{2} < a$ were found to be similar to those previously published [9]. Since the ionic radius of Sr is greater than that of Ca (for twelve-fold oxygen coordination [26, 31] Ca^{2+} (1.34 Å) and Sr^{2+} (1.44 Å)), increasing doping of Sr results in a monotonic increase of the unit cell volume. It appears that c increases more steeply than a and b, and for $y = 0.2$ the lattice parameters are $a \approx b\sqrt{2} \approx c$ [30]. Both the averaged radii of the A-site cations, r_A, and the disorder parameter increase significantly with increasing Sr doping; see figure 1.

Cylinder-shaped samples having a diameter of 1 mm and height of 4.0 mm were used for measurements of the magnetization under hydrostatic pressure. The measurements, using a PAR (Model 4500) vibrating sample magnetometer, were performed in the temperature range 5–250 K and magnetic fields up to 16 kOe, applied perpendicularly to the rotation axis of the samples. The experimental procedures of the magnetic measurements under high hydrostatic pressure are described in detail elsewhere [23–25]. The measurements of ac susceptibility

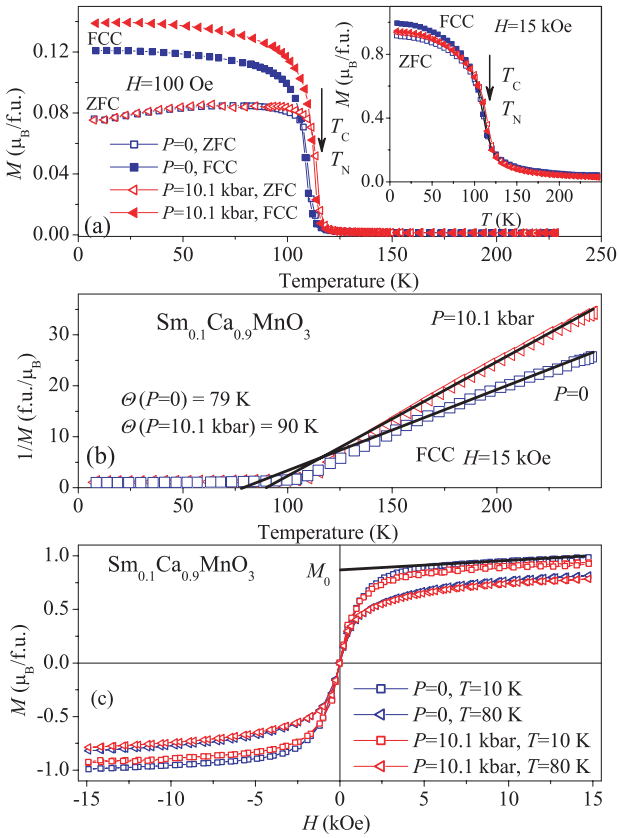

Figure 2. (a) Temperature dependence of zero field cooled M_{ZFC} and field cooled M_{FCC} magnetization of $Sm_{0.1}Ca_{0.9}MnO_3$ at $P = 0$ kbar and at $P = 10.1$ kbar in a magnetic field $H = 100$ Oe. The inset shows M_{ZFC} and M_{FCC} at $P = 0$ kbar and at $P = 10.1$ kbar in a magnetic field $H = 15$ kOe. (b) $1/M$ versus temperature curves for $Sm_{0.1}Ca_{0.9}MnO_3$ at $P = 0$ kbar and at $P = 10.1$ kbar. The solid lines are guides to the eye. (c) Field dependence of magnetization at 10 and 80 K under $P = 0$ kbar and at $P = 10.1$ kbar.

were performed using the magnetic option of the Physical Property Measurement System of Quantum Design.

3. Results

Measurements of the temperature dependences of the magnetization of $Sm_{0.1}Ca_{0.9-y}Sr_yMnO_3$ samples were performed according to the following procedure: the samples were cooled at zero magnetic field to $T = 5$ K, and the magnetization M was measured upon heating (ZFC curve) and immediately thereafter upon cooling (FCC curve) under an applied magnetic field. Figure 2(a) presents the results obtained for $Sm_{0.1}Ca_{0.9}MnO_3$ in a magnetic field of $H = 100$ Oe. It is worth noting that FCC magnetization below the transition temperature increases significantly under pressure, whereas ZFC magnetization remains practically unchanged under an applied pressure. The inset in this figure shows the temperature dependences of the magnetization for $H = 15$ kOe. In agreement with previous studies [9, 10], the magnetization on cooling shows a sharp rise at a well-defined transition temperature of 110 K and two

coexisting phases, ferromagnetic and antiferromagnetic, appear simultaneously. Therefore, we describe the transition temperature by T_C or by T_N, where the abbreviations represent the Curie and the Néel temperatures, respectively. It was found that the pressure coefficient of $Sm_{0.1}Ca_{0.9}MnO_3$ is $dT_C/dP \approx 0.5$ K kbar^{-1}, similar to the results obtained recently from measurements of magnetic susceptibility [27]. The gap between the ZFC and FCC curves observed in $H = 100$ Oe and even in $H = 15$ kOe (the inset in figure 2(a)) is suppressed at an applied pressure of 10.1 kbar and $H = 15$ kOe. The plot of $1/M$ versus T of the FCC values in 15 kOe is given in figure 2(b). For $T > T_C$, the curves obey the Curie–Weiss relation $1/M = (T - \Theta)/CH$ with the Curie–Weiss constant, C, decreasing with increasing pressure, and the paramagnetic Curie temperature, Θ, changing from 79 K for $P = 0$ to 90 K for $P = 10.1$ kbar. This means that the effective FM interactions are enhanced under pressure. Figure 2(c) shows the magnetization of $Sm_{0.1}Ca_{0.9}MnO_3$ versus magnetic fields at 10 and 80 K, under $P = 0$ and 10.1 kbar. Interestingly, the spontaneous magnetization obtained by a linear extrapolation of the high-field magnetization to $H = 0$ ($M_0 \approx 0.86$ μ_B/f.u. at $P = 0$ and $T = 10$ K) decreases slightly with increasing pressure to a value of $M_0 \approx 0.81$ μ_B/f.u. at $P = 10.1$ kbar and $T = 10$ K, in contrast to the behaviour for $La_{0.1}Ca_{0.9}MnO_3$ [29]. The coercive field, H_C, is very small for both temperatures 10 and 80 K, and does not change with pressure; see figure 2(c). Low Sr doping of $y = 0.02$ affects the magnetic characteristics very slightly. It lowers slightly the Curie and Néel temperatures and the pressure coefficient $dT_C/dP \approx 0.4$ K kbar^{-1}, while the paramagnetic Curie temperature, $\Theta(P = 0) \approx 79$ K, and the spontaneous magnetization ($M_0 \approx 0.87$ μ_B/f.u. at $P = 0$ and $T = 10$ K) remain almost unchanged.

The sample with $y = 0.06$ exhibits various metastable magnetic states upon cooling [32], therefore only measurements at ambient pressure were performed. The ZFC and FCC curves at $P = 0$, shown in figure 3(a), are in general very similar to those of $Sm_{0.1}Ca_{0.9}MnO_3$, though its magnetic transition temperature ($T_N \approx T_C \approx 103$ K) and the spontaneous magnetization ($M_0 \approx 0.77$ μ_B/f.u. at $P = 0$ and $T = 10$ K) are lower; see figure 3(a) and the inset to this figure. The ac susceptibility of this sample also resembles that of $Sm_{0.1}Ca_{0.9}MnO_3$ [10], namely χ' exhibits a pronounced peak in the vicinity of T_C and a large bump at $T_m < T_C$, which shifts to higher temperature with increasing frequency; see figure 3(b). Such a frequency-dependent temperature shift is reminiscent of spin-glass-like behaviour, can be attributed to relaxation phenomena in the spin system and can be characterized by the factor $K = \Delta T_m/T_m\Delta(\log\omega)$, where T_m refers to the temperature of the maximum of χ' and ΔT_m is the temperature shift at a given frequency difference. The calculated K factor for the $y = 0.06$ sample is 0.016, falling in the range of values typical for spin glasses [33]. The curves χ' recorded at different ac fields clearly demonstrate nonlinear features, characteristic for spin glasses (figure 3(c)).

Figure 4(a) shows the results obtained for M_{ZFC} and M_{FCC} of $Sm_{0.1}Ca_{0.8}Sr_{0.1}MnO_3$ versus temperature at $P = 0$ and 9.4 kbar in a magnetic field of $H = 100$ Oe. Similarly to the results obtained for $Sm_{0.1}Ca_{0.9}MnO_3$ ([8–10] and figure 2), one may conclude that the sharp rise in the magnetization at about 100 K, recorded on cooling, is attributed to the critical temperature $T_C \approx 100$ K [9, 10]. Note that both $M_{ZFC}(T)$ and $M_{FCC}(T)$ at $P = 0$ display a local minimum at around $T \approx 80$ K that disappears at $P = 9.4$ kbar. The magnetic transition temperature T_C increases under pressure with a pressure coefficient of $dT_C/dP \approx 0.5$ K kbar^{-1}; see the inset of figure 4(a). The magnetization $M_{ZFC}(T)$ of $Sm_{0.1}Ca_{0.8}Sr_{0.1}MnO_3$ displays a smooth anomaly at around $T \approx 80$ K and a pronounced gap between $M_{ZFC}(T)$ and $M_{FCC}(T)$ at ambient pressure in a magnetic field of 15 kOe (figure 4(b)). The above features practically disappear at $P = 9.4$ kbar; see figure 4(b). A plot of $1/M$ versus T of the FCC curves at 15 kOe is given in the inset of figure 4(b). Using the Curie–Weiss relation $1/M = (T - \Theta)/CH$ at 120 K $< T <$ 240 K, one obtains $\Theta \approx 67$ K for $P = 0$ and $\Theta \approx 77$ K for $P = 9.4$ kbar.

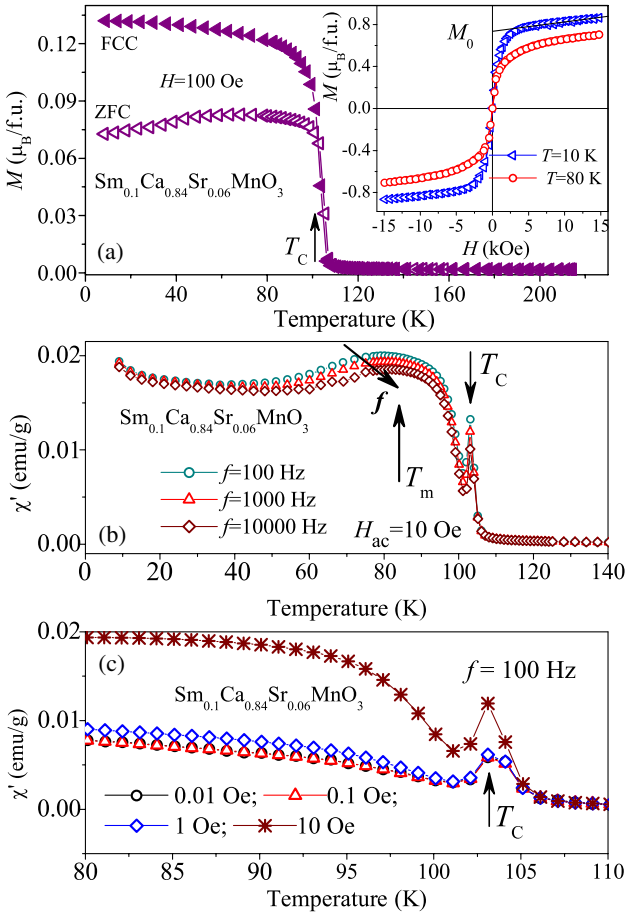

Figure 3. (a) Temperature dependence of zero field cooled M_{ZFC} and field cooled M_{FCC} magnetization of $Sm_{0.1}Ca_{0.84}Sr_{0.06}MnO_3$ at $P = 0$. The inset shows the field dependence of magnetization at 10 and 80 K under $P = 0$. (b) Temperature dependence of ac susceptibility χ' of $Sm_{0.1}Ca_{0.84}Sr_{0.06}MnO_3$ measured at different frequencies 100, 1000 and 10 000 Hz and a magnetic field of 10 Oe; (c) $\chi'(T)$ curves for $Sm_{0.1}Ca_{0.84}Sr_{0.06}MnO_3$ registered at 100 Hz for different excitation fields. The curves corresponding to $H_{ac} = 0.01$ and 0.1 Oe are superimposed.

This means that the effective FM interactions increase under pressure, similarly to that in the case of $Sm_{0.1}Ca_{0.9}MnO_3$; see figure 2(b). One should note that $M(H)$ shows some hysteretic effects, which are suppressed under an applied pressure of 9.4 kbar; see figures 5(a) and (b). The spontaneous magnetization $M_0 \approx 0.58\ \mu_B$/f.u. at $P = 0$ shown in figure 5(a) at $T = 10$ K is attributed to the FM phase. Figure 5(c) shows curves of $M(H)$ at $T = 10$ K under various pressures. It appears that the spontaneous magnetization M_0 increases significantly under small pressures and then approaches a saturation value $M_0 \approx 0.74\ \mu_B$/f.u. at $P \approx 5$ kbar; see inset of figure 5(c).

For the $y = 0.2$ and 0.3 samples, the amount of FM phase is apparently small, thus measurements of both $M_{ZFC}(T)$ and $M_{FCC}(T)$ were performed under a relatively high field of $H = 15$ kOe; see figure 6. The behaviour of $M_{ZFC}(T)$ and $M_{FCC}(T)$ for both samples appears to be quite similar. Both exhibit a pronounced maximum upon cooling (at 125 and 152 K for $y = 0.2$ and 0.3, respectively) accompanied by a sudden drop in magnetization.

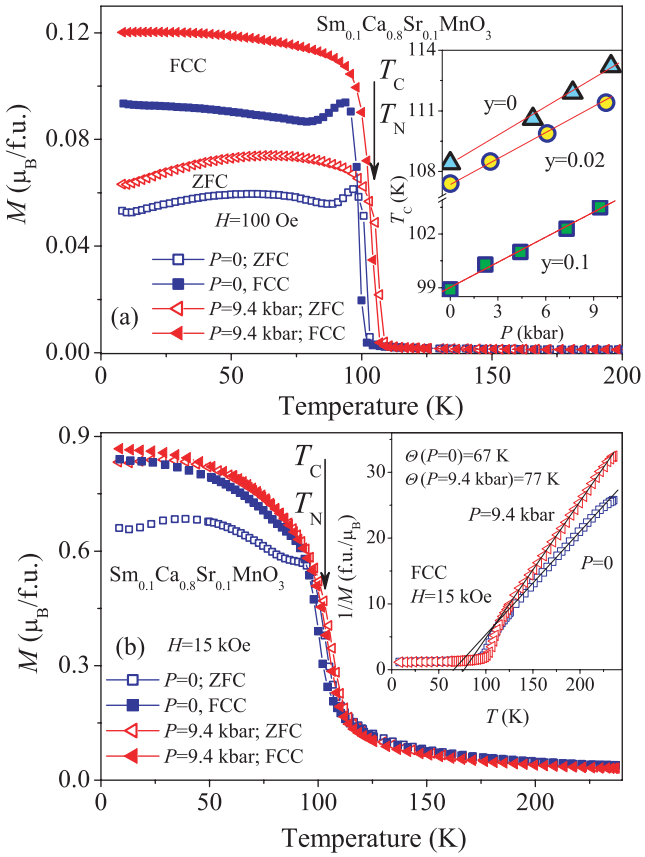

Figure 4. (a) Temperature dependence of zero field cooled M_{ZFC} and field cooled M_{FCC} magnetization of $Sm_{0.1}Ca_{0.8}Sr_{0.1}MnO_3$ at $P = 0$ kbar and at $P = 9.4$ kbar in a magnetic field of $H = 100$ Oe. The inset shows the pressure dependence of T_C for $y = 0$, 0.02 and 0.1 samples; (b) M_{ZFC} and M_{FCC} curves for $Sm_{0.1}Ca_{0.8}Sr_{0.1}MnO_3$ at $P = 0$ kbar and at $P = 9.4$ kbar in a magnetic field of $H = 15$ kOe. The inset shows $1/M$ versus temperature curves for $Sm_{0.1}Ca_{0.8}Sr_{0.1}MnO_3$ at $P = 0$ kbar and $P = 9.4$ kbar. The solid lines are guides to the eye.

These maxima in $M(T)$ are reminiscent of the magnetization peaks found in charge/orbital ordered systems such as $Sm_{1-x}Ca_xMnO_3$ ($x = 0.8$; 0.85) [8], $La_{0.2}Ca_{0.8}MnO_3$ [13, 19], half-doped $Nd_{0.5}Ca_{0.5}MnO_3$, and $Sm_{0.5}Ca_{0.5}MnO_3$ [34]. Upon further cooling, slight increase in the magnetization at about 70 K was observed for both samples; see figure 6. According to neutron diffraction (ND) data [30] for $Sm_{0.1}Ca_{0.6}Sr_{0.3}MnO_3$, the maximum in $M_{ZFC}(T)$ and $M_{FCC}(T)$ dependences at 152 K (figure 6(b)) is attributed to a magnetic transition from paramagnetic to a C-type AFM state, while the kink at around 70 K corresponds to the formation of a G-type AFM phase. Comparing the behaviour of $M_{ZFC}(T)$ and $M_{FCC}(T)$ dependences for both $y = 0.2$ and 0.3 samples (figures 6(a) and (b)), we may suggest that, in the $y = 0.2$ sample, the magnetic transitions to C-type AFM and G-type AFM states occur at 125 and 70 K, respectively. The following features are also noticeable: (i) $M(H)$ does not show a spontaneous moment at $T > 70$ K; (ii) both samples exhibit a very small spontaneous magnetic moment M_0 ($M_0 \approx 0.008$ and $M_0 \approx 0.006$ μ_B/f.u. for $y = 0.2$ and 0.3, respectively) and similar coercive fields of about 1.8 kOe at $T = 10$ K; (iii) an applied pressure suppresses the magnetization in the temperature range 10–250 K. It was found that the position of high-

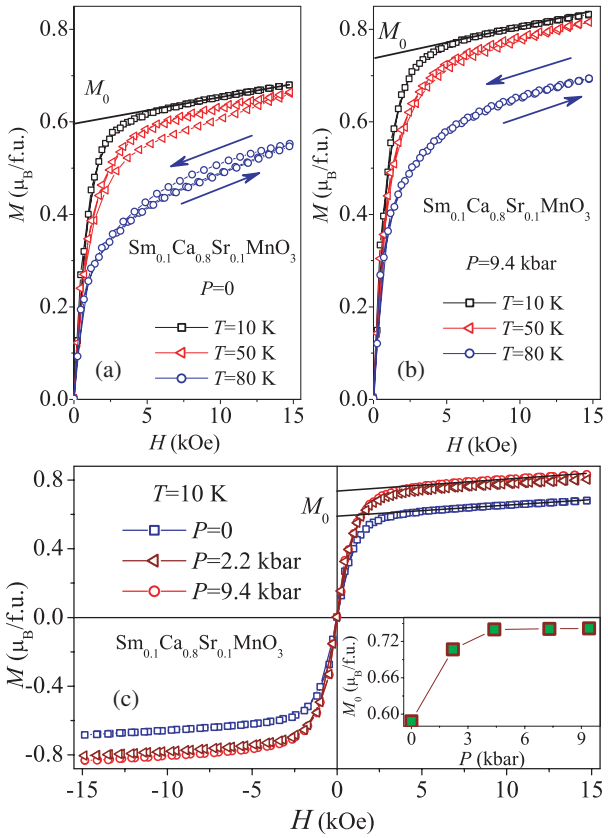

Figure 5. (a) Field dependence of magnetization of $Sm_{0.1}Ca_{0.8}Sr_{0.1}MnO_3$ at various temperatures below T_C under $P = 0$; (b) field dependence of magnetization at various temperatures below T_C under $P = 9.4$ kbar; (c) field dependence of magnetization at $T = 10$ K and various pressures. The inset shows the pressure dependence of spontaneous magnetization at $T = 10$ K.

temperature peaks does not change under pressure, while a rough estimation shows that the low-temperature magnetic transition shifts under pressure towards higher temperatures with a pressure coefficient of ∼0.4 K kbar^{-1}. A comparison of $M(H)$ recorded at 10 K at ambient pressure and at $P = 10.6$ kbar shows that, while M_0 decreases only slightly under an applied pressure, the values of dM/dH are significantly affected by pressure; see inset to figure 6(a).

4. Discussion

Although the spontaneous magnetization M_0 was obtained by a linear extrapolation of the high-field magnetization to $H = 0$ and may give only an estimation of the relative amount of the FM phase, such an evaluation may be very useful in the follow-up for the changes in the FM fraction with Sr doping. On the other hand, we notice that the value of $M_0 \approx 0.86\ \mu_B$/f.u. at $T = 10$ K for $Sm_{0.1}Ca_{0.9}MnO_3$ (figure 2(c)) correlates well with the average magnetic moment at 10 K refined for the FM component from the analysis of the high-resolution ND patters [9] (≈0.9 μ_B/f.u.). Although all samples under investigation have the same carrier concentration of 0.1 electron per Mn ion, they can be divided into two groups, depending on the level of Sr doping. Members of the first group ($0 \leqslant y \leqslant 0.1$) exhibit large enough

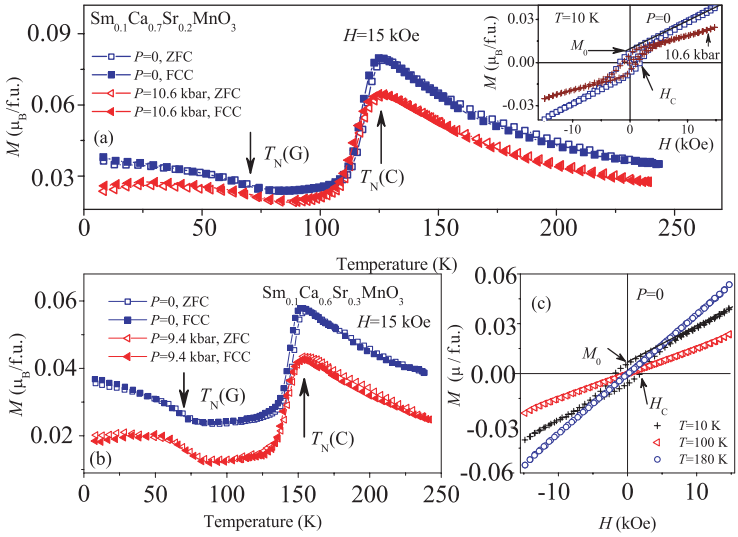

Figure 6. (a) Temperature dependence of M_{ZFC} and M_{FCC} of $Sm_{0.1}Ca_{0.7}Sr_{0.2}MnO_3$ at $P = 0$ kbar and 10.6 kbar in a magnetic field of $H = 15$ kOe. The inset shows the field dependence of magnetization at $T = 10$ K under $P = 0$ kbar and at $P = 10.6$ kbar. (b) Temperature dependence of M_{ZFC} and M_{FCC} of $Sm_{0.1}Ca_{0.6}Sr_{0.3}MnO_3$ at $P = 0$ kbar and at $P = 9.4$ kbar in a magnetic field of $H = 15$ kOe. (c) Field dependence of magnetization of $Sm_{0.1}Ca_{0.6}Sr_{0.3}MnO_3$ at $P = 0$ kbar for various temperatures.

spontaneous magnetic moment $M_0 > 0.5\ \mu_B$/f.u. at low temperatures; see figure 7. Since the theoretical spin value for all samples is 3.1 μ_B/Mn site, we may conclude by a rough estimation that the volume of the FM phase at 10 K, which approximately corresponds to the M_0 value, varies from about 28% for $Sm_{0.1}Ca_{0.9}MnO_3$ and $Sm_{0.1}Ca_{0.88}Sr_{0.02}O_3$ samples to about 18% in $Sm_{0.1}Ca_{0.8}Sr_{0.1}O_3$. On the other hand, the relative volume of the FM phase for the samples of the second group is very small (<0.3% for $y = 0.2$ and 0.3 samples). The Curie temperature T_C and the paramagnetic Curie–Weiss temperature Θ decrease slightly for $y > 0.02$, pointing out that not only the volume of the FM phase diminishes with increasing y but also the DE interaction decreases with increasing Sr doping as well; see figures 2–4. Chmaissem *et al* [35] have revealed that the behaviour of the Néel temperature T_N in the $Ca_{1-x}Sr_xMnO_3$ system can be described satisfactory as a function $T_N \sim \langle\cos^2\phi\rangle$, where angle ϕ characterizes a bending of the $(180° - \phi)$ Mn–O–Mn bond angle. Zhou and Goodenough [36] have also studied the variation of the Néel temperature with pressure for the orbitally ordered $Mn(III)O_3$ array in the family of single-valent $RMnO_3$ (R = La, Pr, Sm) and for the $Mn(IV)O_3$ array in $Ca_{1-x}Sr_xMnO_3$. They have suggested that the above empirical relationship for the Néel temperature found for the orthorhombic structure provides evidence for the dominance of the semicovalent-exchange term over the superexchange term. It appears that a possible reason for the decrease in T_N with Sr doping for orthorhombic $Sm_{0.1}Ca_{0.9-y}Sr_yMnO_3$ ($0 < y < 0.1$) may also stem from a decrease in the bending angle. On the other hand, the above relationship does not hold for $LaTiO_3$, in which T_N decreases as the bending angle increases [36].

As already noted, the temperature dependences of the magnetization for $Sm_{0.1}Ca_{0.9-y}Sr_y$ MnO_3 ($0 \leqslant y \leqslant 0.1$) show a large difference between M_{ZFC} and M_{FCC} curves below T_C (figures 2–4), similar to that observed previously for $La_{0.1}Ca_{0.9}MnO_3$ [19]. Generally, the difference between the M_{FCC} and M_{ZFC} in manganites is caused by a 'freezing' of the magnetic moments in directions energetically favoured by their local anisotropy or by the external field

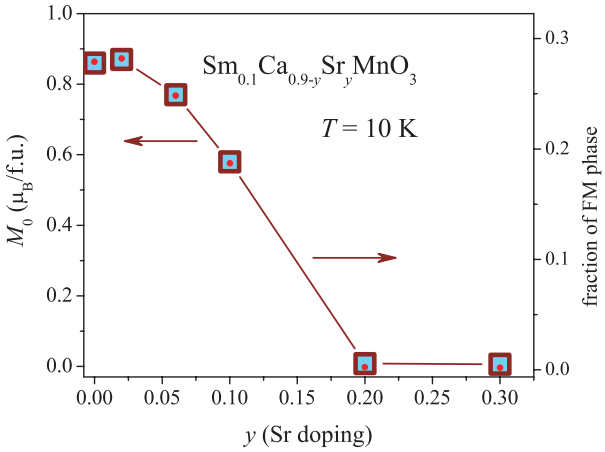

Figure 7. Variation of spontaneous magnetization with Sr doping and fraction of the FM phase at $T = 10$ K in the $Sm_{0.1}Ca_{0.9-y}Sr_yMnO_3$ system.

and may be a manifestation of FM cluster glass behaviour [1, 2, 10]. It appears that, at a high enough density of FM clusters in $Sm_{0.1}Ca_{0.9-y}Sr_yMnO_3$ ($0 \leqslant y \leqslant 0.1$), samples below T_C exhibit the features typical of an FM cluster glass, namely a gap between the FCC and ZFC magnetization curves and a frequency shift of the ac susceptibility [10, 28]; see figures 2–4.

The results of detailed combined neutron powder diffraction and magnetization studies [13, 14] of electron-doped $Ca_{1-x}La_xMnO_3$ ($0 \leqslant x \leqslant 0.2$) suggest that La doping in $CaMnO_3$ leads to the formation of nanometric-scale FM clusters which are isolated for sufficiently low doping ($x < 0.05$). For intermediate doping ($x \sim 0.1$), a canting of a G-AFM spin matrix, where FM clusters are embedded, takes place. The density of the FM clusters of $\sim$1 nm in size, as well as the FM component of the canted state, increases with the doping level and, at some level of doping overall, the FM moment becomes dominant over the G-AFM spin component [14]. Although, on substitution of Ca by Sr, the carrier concentration remains constant, the variation in the bending angle of the Mn–O–Mn bond with Sr doping may affect the canted state of the G-AFM structure and the decrease in the canting angle with y may also be responsible for the progressive diminution of the FM component with increasing doping; see figures 2–4.

One should note that the hysteresis loops for samples of both groups are also significantly different at low temperatures; see figures 2, 3, 5, 6. It has been concluded previously [16, 37] that there are two possible contributions to the magnetization: polarization of FM clusters and spin canting of the AFM spin structure, while the coercivity occurs due to an exchange-type coupling between the FM clusters and an AFM matrix. Hysteresis loops (see figures 2, 3, 5 and 6) show that a considerable coercive field of $H_C \approx 1.8$ kOe occurs only for the samples with a low volume of the FM phase ($y = 0.2$ and 0.3—figure 6). In this case, the interfacial spins between the FM and AFM regions tend to rotate with the FM clusters, but experience an increased rotational drag due to the AFM matrix, leading to a broadening of the hysteresis loops (figure 6) [17]. For samples of the first group, the sizes of the FM clusters increase significantly, thus reducing the dragging and the coercive force considerably; see figures 2, 3 and 5.

Maignan *et al* [16] have shown that, in electron-doped $RE_{1-x}Ca_xMnO_3$ (RE = Pr, Nd, Gd, Eu, Ho), the value of x_{max}, at which the amount of FM phase maximizes, shows a sharp maximum that depends on r_A and the cation size disorder. It was found [17] that an increase in r_A and σ^2 from Y^{3+} (1.19 Å) to La^{3+} (1.29 Å) results in a shift of x_{max} from 0.85 to 0.93.

In hole-doped manganites, an increase in the volume of the FM phase and T_C is accompanied in general by increasing r_A [1, 2]. For electron-doped $Sm_{0.1}Ca_{0.9-y}Sr_yMnO_3$, an increase in Sr doping followed by an increase in r_A and σ^2 (figure 1) results in almost full suppression of ferromagnetism at $y \geqslant 0.2$; see figures 6 and 7. A similar suppression of ferromagnetism with increasing Sr doping has been observed previously for $La_{0.1}Ca_{0.9-y}Sr_yMnO_3$, in which Sr doping of $y = 0.1$ reduces the saturation moment M_S to 0.1 of the M_S value observed for $y = 0$; see [14]. Following this study and results obtained in recent ND studies for $Sm_{0.1}Ca_{0.6}Sr_{0.3}MnO_3$ [30], the high-temperature peaks of the magnetization (figures 6(a), (b)) may be associated with the orbital ordering (OO) transition. The ND studies [30] of $Sm_{0.1}Ca_{0.6}Sr_{0.3}MnO_3$ have indicated few significant features. (i) At $T \approx 150$ K, a structural phase transition to a monoclinic unit cell occurs. The above structural transition occurs concurrently with the appearance of a C-type AFM magnetic structure at $T_N(C)$; its ordered magnetic moment, $\mathbf{m}(C)$, reaches a value of about 2 μ_B per Mn ion at $T < 20$ K. (ii) At lower temperature, a transition to a G-AFM structure occurs at $T_N(G) \approx 70$ K, and $\mathbf{m}(G)$ reaches a value of about 1.1 μ_B/Mn at $T < 5$ K. One can conclude from figure 6(c) that the weak FM component is superimposed on the G-AFM structure. Thus, the results presented in figure 6, combined with ND data [30], indicate a coexistence of C-AFM regions with no FM moment and regions with coupled G-AFM + FM moments for $Sm_{0.1}Ca_{0.9-y}Sr_yMnO_3$ ($y = 0.2, 0.3$).

The marked minimum seen around 85 K in the ZFC and FCC curves at ambient pressure (figure 4(a)) and the pronounced hysteresis of the $M(H)$ curves in the case of $Sm_{0.1}Ca_{0.8}Sr_{0.1}MnO_3$ (figure 5(a)) resemble the behaviour of $La_{0.1}Ca_{0.9}MnO_3$ [29]. It was suggested in the case of $La_{0.1}Ca_{0.9}MnO_3$ that such effects may arise due to strong competition between different magnetic and crystallographic structures, because $La_{0.1}Ca_{0.9}MnO_3$ exhibits a structural phase transition followed by two magnetic transitions at T_N (C-AFM) $\approx$ $T_N(G$-AFM) $\approx$ 108 K. The results of magnetic measurements obtained for $La_{0.1}Ca_{0.9}MnO_3$ may indicate that the source of the hysteretic effects is related to a field-induced change in the ratio between C-AFM-$P2_1/m$ and G-AFM + FM-$Pnma$ phases, certainly favouring the G-AFM + FM-$Pnma$ phase at the expense of the C-AFM-$P2_1/m$ phase [38]. This effect was found to be relatively small at low temperatures ($T \ll T_N$) and increases with increasing temperature ($T < T_N$), where competing phases have comparable energies [29]. A remarkable magnetic hysteresis was observed for $Sm_{0.1}Ca_{0.8}Sr_{0.1}MnO_3$ at 80 and 50 K (figure 5(a)), but it is absent at 10 K, and is similar to the magnetic behaviour of $La_{0.1}Ca_{0.9}MnO_3$ [29]. It is worth noting that an applied pressure of 9.4 kbar affects the temperature and field dependences of magnetization (figures 4 and 5) in the following way: it suppresses the marked minimum observed at $H = 100$ Oe in both the ZFC and FCC curves (figure 4(a)) and diminishes the hysteretic effect in $M(H)$ loops (figure 5(b)). The application of pressure also results in an increase in M_0 (see figure 5(c) and the inset to figure 5(c)) at $T = 10$ K. One should note that this effect is more pronounced at a relatively low applied pressure of $P < 3$ kbar, while for $P > 5$ kbar, M_0 practically does not depend any more on pressure. As mentioned previously [20], two mechanisms may play significant roles here: (i) an increase in the volume of the FM droplets, inside the G-AFM matrix and; (ii) an increase in the canting angle of the G-AFM moments.

It is worth noting that samples of the first group with $y = 0$, 0.02 and 0.06 do not exhibit a minimum in ZFC and FCC and do not show hysteretic behaviour in the $M(H)$ dependences. This fact may also be understood in the frame of phase competition. As already pointed out, $Sm_{0.1}Ca_{0.9}MnO_3$ preserves its $Pnma$ regular structure and exhibits only a G-AFM magnetic structure with a relative large FM component, almost maximal in the $Sm_{1-x}Ca_xMnO_3$ system [8]. The magnetic interactions (characterized by T_C, Θ; see figures 2–4) and the volume of the FM phase (characterized by M_0—figure 7) maintain almost the same values for $y = 0$,

0.02 and 0.06, possibly due to preserving a unique G-AFM+ FM-$Pnma$ phase. For these samples, the effect of applied pressure on the FM phase is very small (see figure 2). An additional doping ($y = 0.1$ case) may yield a competing C-AFM-$P2_1/m$ phase, developed with increasing Sr doping and becoming predominant for $y \geqslant 0.2$. Possibly, this is the main reason for diminution of the magnetic interactions and for a decrease in the volume of the FM phase in this doped manganite. Additional extensive studies of the crystallographic and magnetic structure of the $y = 0.1$ sample over a wide temperature range, from low temperature up to room temperature, are entirely needed for an understanding of the variation of magnetic and structural phases with Sr doping,

The effect of applied pressure on the magnetic transition temperature shows that the pressure coefficient $\mathrm{d}T_C/\mathrm{d}P \approx 0.4$–$0.5$ K kbar^{-1} observed for all samples with $0 \leqslant y \leqslant 0.1$ is similar to that found previously for electron-doped $La_{1-x}Ca_xMnO_3$ [20], $Y_{1-x}Ca_xMnO_3$ [19] and $Sm_{1-x}Ca_xMnO_3$ [19] ($x \sim 0.9$) with competing FM and AFM phases. It has been well established that magnetic and transport properties of manganites are essentially determined by the bandwidth W, described by the expression [39]: $W \sim \cos\omega/(d_{\mathrm{Mn-O}})^{3.5}$, where ω is the tilt angle in the plane of the bond and $d_{\mathrm{Mn-O}}$ is the Mn–O bond length. In the case of a strong Hund's coupling effective for manganites, $J_H \gg W$ and $T_C \propto W$ [40]. In the absence of Jahn–Teller distortion of the MnO_6 octahedron (in $Sm_{0.1}Ca_{0.9-y}Sr_yMnO_3$ samples, only 10% of Mn ions are Jahn–Teller active Mn^{3+}), the bandwidth W is determined by the hopping integral t of e_g electrons. Using the results obtained by Sacchetti *et al* [41], one may express the variation of the hopping integral in the range of modest pressure by an empirical expression: $t(P) = t(0)[1 + 0.001P(\mathrm{kbar})]$. Taking into account the proportionality between t and T_C at $P = 0$, one may conclude that the increase in the hopping integral due to variation of structural parameters alone corresponds to values $\mathrm{d}T_C/\mathrm{d}P \approx 0.2$ K kbar^{-1} [1, 2, 18–21]. It is known [1, 2, 19–26] that the hole-doped manganites with an FM metallic ground state in general exhibit a pressure coefficient of $\mathrm{d}T_C/\mathrm{d}P \approx (1.5$–$2)$ K kbar^{-1}. Nevertheless, the above value of 0.2 K kbar^{-1} is comparable with the values observed for electron-doped manganites. Moreover, the reduction of electron–phonon coupling under pressure may also be essential, especially in the low-pressure regime [41].

Samples with $y = 0.2$ and 0.3 exhibit quite different magnetic characteristics under pressure. For these samples, an applied pressure does not practically affect the magnetic transition temperatures $T_N(C)$ and increases slightly only $T_N(G)$ (see figure 6), but strongly suppresses the magnetization at all temperatures. Recently, we observed a reduction in the magnetization in electron-doped $La_{0.2}Ca_{0.8}MnO_3$ in the paramagnetic region (at temperatures greater than both the temperature of orbital ordering and the temperature of AFM ordering at $T_N < T_{OO} \approx 215$ K) [29]. Pissas *et al* [11] have suggested that the broad magnetization peak in the vicinity of the orbital ordering transition in $La_{0.2}Ca_{0.8}MnO_3$ may be attributed to the hopping of the e_g electrons, which brings the FM correlations through the DE mechanism. At lower temperatures, the e_g electrons 'freeze' and the FM fluctuations are replaced by a superexchange-driven AFM spin configuration. The reduction in the spontaneous magnetization M_0, the decrease in slope of $M(H)$, and the shift of the $T_N(G\text{-AFM})$ towards higher temperatures under an applied pressure (figure 6) are indicative of an enhancement of the AFM interactions in $y = 0.2$ and 0.3 samples at the expense of the FM interactions.

5. Conclusions

In conclusion, we have found that low-Sr-doped $Sm_{0.1}Ca_{0.9-y}Sr_yMnO_3$ ($y = 0$–0.1) samples exhibit magnetic phase separation below $T_C \approx 100$–110 K, consisting of ferromagnetic clusters embedded in an antiferromagnetic G-AFM type matrix. The volume of the FM phase at 10 K

decreases progressively with increasing Sr doping from 28% ($y = 0$) to 18% ($y = 0.1$). It was found that, for all samples with $y = 0$–0.1, an applied pressure enhances T_C with a pressure coefficient of $dT_C/dP \approx 0.4$–0.5 K kbar^{-1}. Hysteretic effects in the $M(H)$ dependences of $Sm_{0.1}Ca_{0.8}Sr_{0.1}MnO_3$ manifest significant competition between the FM and the AFM components in the G-type AFM structure. An applied pressure increases the volume of the FM phase significantly for the $y = 0.1$ sample. The behaviour of the $y = 0.2$ and 0.3 Sr-doped manganites is quite different; they exhibit a heterogeneous spin configuration in their ground state C-AFM (at ≈125 K and ≈152 K for $y = 0.2$ and 0.3, respectively) and a G-AFM phase with a very weak FM moment (at ≈70 K for both samples) associated with two magnetic transitions in their ordered magnetic structures. For these compounds, the temperature $T_N(C)$ of the transition from a paramagnetic to a C-AFM magnetic structure is practically insensitive to an applied pressure, while $T_N(G)$ slightly increases under pressure. It was also found that, for both samples, an applied pressure decreases significantly the FM correlations in the paramagnetic state (at $T > T_N(C)$) as well as the FM component at low temperatures.

Acknowledgment

This work was supported in part by the Polish State Committee for Scientific Research under research project no. 1 P03B 123 30.

References

[1] Dagotto E 2003 *Nanoscale Phase Separation and Colossal Magnetoresistance* (*Springer Series in Solid State Physics* vol 136) (Berlin: Springer)
[2] Goodenough J B 2003 Rare earth manganese perovskites *Handbook on the Physics and Chemistry of Rare Earth* vol 33, ed K A Gschneidner Jr, J-C G Bunzli and V K Pecharsky (Amsterdam: Elsevier Science)
[3] Moreo A, Mayr M, Feiguin A, Yunoki S and Dagotto E 2000 *Phys. Rev. Lett.* **84** 5568
[4] Uehara M, Mori S, Chen C H and Cheong S-W 1999 *Nature* **399** 560
[5] Burgy J, Moreo A and Dagotto E 2004 *Phys. Rev. Lett.* **92** 097202
[6] Tomioka Y and Tokura Y 2002 *Phys. Rev.* B **66** 104416
[7] Rodriguez-Martinez L M and Attfield J P 1998 *Phys. Rev.* B **54** R15622
[8] Martin C, Maignan A, Hervieu M and Raveau B 1999 *Phys. Rev.* B **60** 12191
[9] Martin C, Maignan A, Hervieu M, Raveau B, Jirák Z, Savosta M M, Kurbakov A, Trounov V, André G and Bourée F 2000 *Phys. Rev.* B **62** 6442
[10] Maignan A, Martin C, Damay F, Raveau B and Hejtmanek J 1998 *Phys. Rev.* B **58** 2758
[11] Pissas M, Kallias G, Hofmann M and Többens D M 2002 *Phys. Rev.* B **65** 064413
[12] Pissas M and Kallias G 2003 *Phys. Rev.* B **68** 134414
[13] Ling C D, Granado E, Neumeier J J, Lynn J W and Argyriou D N 2003 *Phys. Rev.* B **68** 134439
[14] Granado E, Ling C D, Neumeier J J, Lynn J W and Argyriou D N 2003 *Phys. Rev.* B **68** 134440
[15] Fujishiro H, Ikebe M, Ohshiden S and Noto K 2000 *J. Phys. Soc. Japan* **69** 1865
[16] Maignan A, Martin C, Damay F and Raveau B 1998 *Chem. Mater.* **10** 950
[17] Sudheendra L, Raju A R and Rao C N R 2003 *J. Phys.: Condens. Matter* **15** 895
[18] Respaud M, Broto J M, Rakoto H, Vanacken J, Wagner P, Martin C, Maignan A and Raveau B 2001 *Phys. Rev.* B **63** 144426
[19] Neumeier J J, Hundley M F, Thompson J D and Heffner R H 1995 *Phys. Rev.* B **52** R7006
[20] Hwang H Y, Palstra T T M, Cheong S-W and Batlogg B 1995 *Phys. Rev.* B **52** 15046
[21] De Teresa J M, Ibarra M R, Blasco J, Garcia J, Marquina C, Algarabel P A, Arnold Z, Kamenev K, Ritter C and von Helmolt R 1996 *Phys. Rev.* B **54** 1187
[22] Okuda T, Tomioka Y, Asamitsu A and Tokura Y 2000 *Phys. Rev.* B **61** 8009
[23] Markovich V, Fita I, Puzniak R, Tsindlekht M I, Wisniewski A and Gorodetsky G 2002 *Phys. Rev.* B **66** 094409
[24] Markovich V, Fita I, Puzniak R, Wisniewski A, Suzuki K, Cochrane J W, Yuzhelevski Y, Mukovskii Ya M and Gorodetsky G 2005 *Phys. Rev.* B **71** 224409

[25] Baran M, Dyakonov V, Gladczuk L, Levchenko G, Piechota S and Szymczak H 1995 *Physica* C **241** 383
[26] Coey J M D, Viret M and von Molnar S 1999 *Adv. Phys.* **48** 167
[27] Garbarino G, Acha C, Vega D, Leyva G, Polla G, Martin C, Maignan A and Raveau B 2004 *Phys. Rev.* B **70** 014414
[28] Markovich V, Fita I, Puzniak R, Rozenberg E, Wisniewski A, Martin C, Maignan A, Hervieu M, Raveau B and Gorodetsky G 2002 *Phys. Rev.* B **65** 224415
[29] Markovich V, Fita I, Puzniak R, Rozenberg E, Martin C, Wisniewski A, Yuzhelevski Y and Gorodetsky G 2005 *Phys. Rev.* B **71** 134427
[30] Martin C, Maignan A, Hébert S, André G, Kurbakov A, Broto J M and Rakoto H 2006 in progress
[31] Shannon R D 1976 *Acta Crystallogr.* A **32** 751
[32] Markovich V, Fita I, Puzniak R, Martin C, Kikoin K, Wisniewski A, Maignan A and Gorodetsky G 2006 *Phys. Rev.* B submitted
[33] Mydosh J A 1993 *Spin Glasses* (London: Taylor and Francis)
[34] López J, de Lima O F, Lisboa-Filho P N and Araujo-Moreira F M 2002 *Phys. Rev.* B **66** 214402
[35] Chmaissem O, Dabrowski B, Kolesnik S, Mais J, Brown D E, Kruk R, Prior P, Pyles P and Jorgensen J D 2001 *Phys. Rev.* B **64** 134412
[36] Zhou J S and Goodenough J B 2003 *Phys. Rev.* B **68** 054403
[37] Muroi M and Street R 1999 *Aust. J. Phys.* **52** 205
[38] Algarabel P A, De Teresa J M, García-Landa B, Morellon L, Ibarra M R, Ritter C, Mahendiran R, Maignan A, Hervieu M, Martin C, Raveau B, Kurbakov A and Trounov V 2002 *Phys. Rev.* B **65** 104437
[39] Medarde M, Mesot M, Lacorre P, Rosenkranz S, Fisher P and Gobrecht K 1995 *Phys. Rev.* B **52** 9248
[40] Furukawa N 1999 *Physics of Manganites* (*Series Fundamental Materials Research*) ed T A Kaplan and S D Mahanti (New York: Kluwer–Academic/Plenum) p 1
[41] Sacchetti A, Postorino P and Capone M 2006 *New J. Phys.* **8** 3